

Special
Collection

Enzymatic S-Methylation of Thiols Catalyzed by Different O-Methyltransferases

Eman Abdelraheem^{+, [a]} Emely Jockmann^{+, [b]} Jianyu Li,^[c] Stefan Günther,^[c] Jennifer N. Andexer,^{*, [b]} Peter-Leon Hagedoorn,^[a] and Ulf Hanefeld^{*, [a]}

S-Adenosyl-L-methionine (SAM)-dependent methyltransferases (MTs) are highly chemoselective enzymes grouped in C-, N-, O-, S- and halide MTs, depending on the (hetero) atom that acts as the methyl group acceptor. So far, OMTs present the largest group, including many well investigated candidates. The catechol OMT from mammals such as from *Rattus norvegicus* (*RnCOMT*) is involved in the metabolism of neurotransmitters like dopamine. It is known to methylate the hydroxyl of the catechol ring in the 3 position. There are also reports showing that the regioselectivity of different COMTs can vary leading to different products with methyl groups in the 3 and/or 4 positions. Nevertheless, there was only O-methylation re-

ported for COMTs. Another related MT, the caffeate OMT involved in the lignin biosynthesis of plants has also been reported as a chemoselective enzyme. In nature, S-methylation is a rare phenomenon with different methyl donors being involved in the methyl transfer onto sulfur atoms. Several SAM-dependent MTs are identified as S-methyltransferases (SMTs), these are involved in salvaging pathways and xenobiotic metabolism of cells. Here, we report a new function of three OMTs; *RnCOMT*, a COMT from *Myxococcus xanthus* (*MxSafC*), and a CaOMT from *Prunus persica* (*PpCaOMT*) with acceptance towards different aromatic thiol substrates with up to full conversion.

Introduction

Selective enzymatic methylation reactions are of great interest for the synthesis of methylated bioactive molecules.^[1–3] In nature, methylation is mainly carried out by S-adenosylmethionine (SAM)-dependent methyltransferases (MTs; EC 2.1.1.—).^[4] Improved enzymatic systems/cascades using stable and inexpensive starting materials are highly promising tools for an environmentally friendly synthesis of methylated bioactive

compounds.^[5–11] They have become a sought-after alternative for standard methylating agents such as methyl iodide and dimethyl sulfate, which are toxic, require the use of organic solvents, and often display no selectivity.^[4,12,13] MTs can be classified as O-, N-, S-, or C-MTs with OMTs being the largest group.^[4]

OMTs have been the focus of research since many years, due to their involvement in metabolic pathways of many different organisms (Figure 1). One example is the catechol OMT (COMT; EC 2.1.1.6), which has been studied in detail since the 1950s.^[14,15] In addition to its main function in mammals, the disposing of neurotransmitters, COMTs have been characterized regarding their substrate range and suitability as biocatalysts for technical applications.^[16,17] Structurally, COMT is a monomeric enzyme featuring a central β -sheet flanked by α -helices on both sides.^[14,18] The proposed mechanism of COMT-catalyzed methylation of catechols in the presence of SAM includes the coordination of Mg^{2+} by the hydroxyl groups of the catechol substrate which lowers their pK_a values; this aids the deprotonation of the hydroxyl group closest to the SAM methyl group by a lysine residue (Figure 2).^[14,19] The broad substrate range of COMTs can be explained by the architecture of the acceptor substrate binding pocket; apart from the Mg^{2+} stabilizing the catechol moiety, the binding site is an open cleft fitting small and large catechol compounds such as 3,4-dihydroxybenzaldehyde and tetrahydroisoquinolines (THIQs), respectively.^[5,14,19–21] COMTs transfer the methyl group with a certain regioselectivity regarding the two hydroxyls of the catechol; this is controlled by the orientation of the functional groups in the active site through a range of structural features.^[21–24] While most mammalian enzymes show *meta* selectivity, *para*-selective enzymes are described as well, e.g., a COMT involved in saframycin biosynthesis in *Myxococcus xanthus* (*MxSafC*). In contrast to the

[a] Dr. E. Abdelraheem,⁺ Dr. P.-L. Hagedoorn, Prof. Dr. U. Hanefeld
Biocatalysis, Department of Biotechnology
Delft University of Technology
Van der Maasweg 9, 2629 HZ Delft (The Netherlands)
E-mail: U.Hanefeld@tudelft.nl

[b] E. Jockmann,⁺ Prof. Dr. J. N. Andexer
Institute of Pharmaceutical Sciences
Pharmaceutical and Medicinal Chemistry
University of Freiburg
Albertstraße 25, 79104 Freiburg (Germany)
E-mail: Jennifer.Andexer@pharmazie.uni-freiburg.de

[c] Dr. J. Li, Prof. Dr. S. Günther
Institute of Pharmaceutical Sciences
Pharmaceutical Bioinformatics
University of Freiburg
Hermann-Herder-Straße 9, 79104 Freiburg (Germany)

[+] both authors contributed equally

Supporting information for this article is available on the WWW under <https://doi.org/10.1002/cctc.202301217>

This publication is part of a joint Special Collection with ChemBioChem published dedicated to the conference Biotrans 2023. Please see our homepage for more articles in the collection.

© 2023 The Authors. ChemCatChem published by Wiley-VCH GmbH. This is an open access article under the terms of the Creative Commons Attribution License, which permits use, distribution and reproduction in any medium, provided the original work is properly cited.

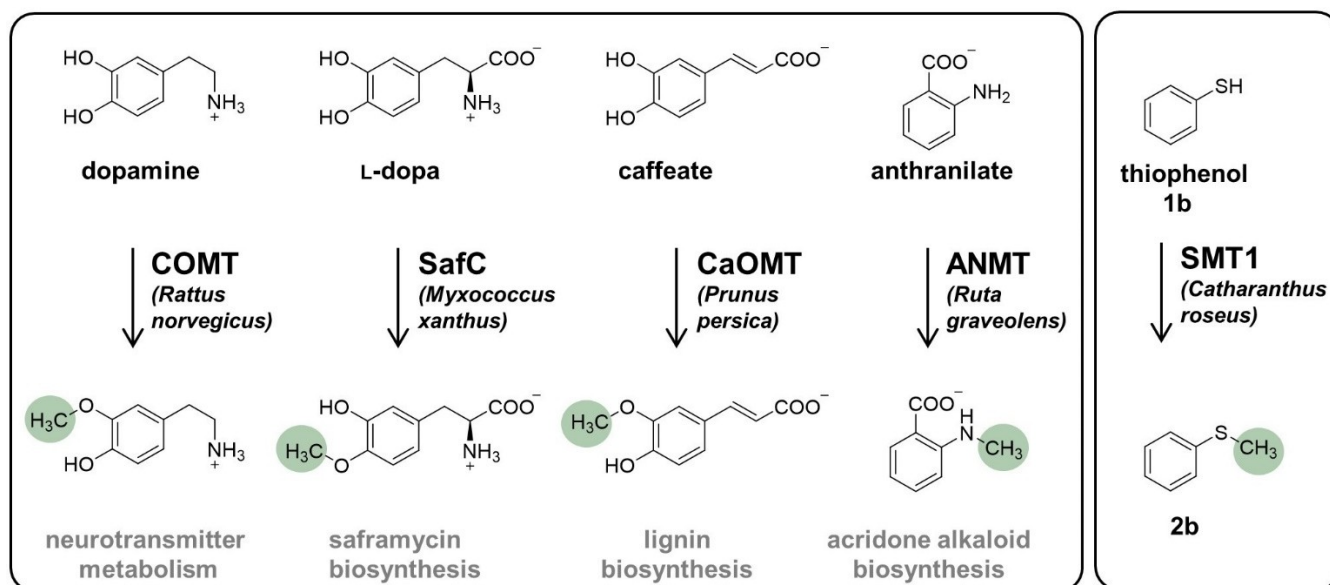


Figure 1. Different MTs and their substrates. *RnCOMT meta* methylates dopamine. The reaction is one possible metabolic step for neurotransmitters in mammals. *MxSafC*, a bacterial catechol OMT is involved in the saframycin biosynthesis, methylating L-dopa in *para* position. The natural substrate of *PpCaOMT* is caffeate, the methylated substrate is a precursor used in the lignin biosynthesis in plants. No natural substrate has been identified for *CrSMT*. It was shown that several thiol containing substrates such as thiophenol were methylated, identifying the enzyme as an SMT.

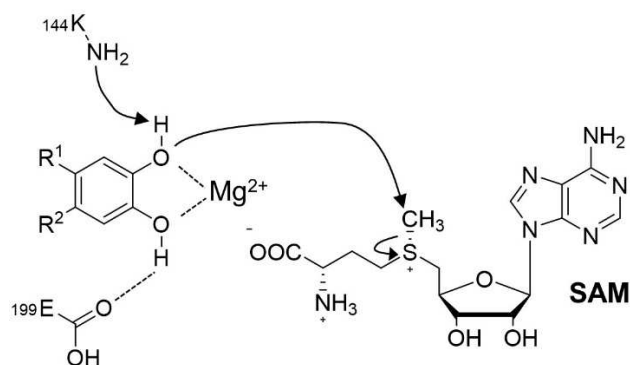


Figure 2. Mechanism of methylation reaction in *RnCOMT*. The catechol substrate coordinates to the Mg^{2+} ion in the active site. Therefore, the pK_a value of the hydroxyl group is decreased followed by a deprotonation step of the hydroxyl group by a lysine residue. The deprotonated hydroxylate being the nucleophile, attacks the methyl group carbon of SAM.

neurotransmitter-disposing COMTs stemming from catabolism, biosynthetic enzymes such as *MxSafC* often show a higher regioselectivity.^[5,24] An example is the methylation of dopamine catalyzed by *RnCOMT* or *MxSafC* that leads to different (main) products. While *RnCOMT* forms the *meta* and *para* methylated products in a ratio of 4:1, *MxSafC* only catalyzes the methylation step in *para* position.^[5] Nevertheless, the regioselectivity has been shown to vary and depends on the particular enzyme, the acceptor substrate used, as well as the assay conditions.^[5,21,22,24] Furthermore, *MxSafC* has also been described to catalyze the dimethylation of THIQs on both catechol hydroxyl groups.^[21]

Another example for a well-known group of OMTs are plant OMTs involved in the biosynthesis of lignin and other natural products.^[25–27] Most of these metal-independent OMTs display a

broad substrate scope; they are reported to methylate many classes of compounds such as eugenol, chavicol, coumarins, flavonoids, isoflavonoids, and polyalcohols, in some cases the corresponding coenzyme A esters are the actual substrates.^[25,26] Small changes in one or a few amino acids are sufficient to modify the substrate specificity for these enzymes.^[27] Furthermore, divergent chemoselectivity has been described: this includes anthranilate NMTs (ANMTs; EC 2.1.1.111) that are (regarding the amino acid sequence) closely related to caffeate OMTs (CaOMTs, >60% similarity; EC 2.1.1.68), but exhibit strict selectivity for *N*-methylation.^[28,29] Another example is *CrSMT1* from *Catharanthus roseus*, an *S*-methyltransferase (SMT) sharing 56–59% identity with CaOMTs, showing only minor structural differences compared to CaOMTs. This enzyme is a promiscuous *S*/*O*-methyltransferase (*S*/OMT) preferring thiol substrates over the corresponding hydroxyl compounds (Figure 1).^[30]

As discussed above, the regioselectivity of OMTs has been studied in detail and is to an extent well understood.^[21,24,29] The focus of the current study is OMT chemoselectivity, for which the molecular details are not as well known. We chose the *S*-selectivity described for *CrSMT1* as a suitable starting point, since both, the hydroxyl and thiol groups are good nucleophiles and could act as methyl acceptors. In general, *S*-methylation is of rare occurrence in nature, and achieved with different strategies: the formation of L-methionine, starting from L-homocysteine, is catalyzed by various enzymes using different methyl donors. L-homocysteine SMTs (HSMTs) use *S*-methyl-L-methionine as cosubstrate, while betaine SMTs (BHMTs) transfer the methyl group from betaine, and L-methionine synthases from 5-methyltetrahydrofolate onto L-homocysteine.^[31–33] Some HSMTs, such as *ScMHT1* from *Saccharomyces cerevisiae*, also accept the non-enzymatic SAM epimerization product (*R,S*)-SAM

as methyl donor, to break down the inactive form of the cofactor, leading to L-methionine for the production of new, active cofactor molecules with (*S,S*)-configuration.^[34] Besides this salvaging step, SAM-dependent *S*-methylation has been described for different organisms including bacteria, microalgae and humans.^[35,36] The thiopurine MT especially being present in liver cells in the human body methylates 6-mercaptopurine, an anticancer drug, used in acute lymphoblastic leukemia therapy.^[36] There is only little information about the physiological functions of the described SAM-dependent SMTs. In general, they seem involved in the metabolism of xenobiotic thiols, the detoxification of poisonous compounds, and the recycling of inactive compounds in cells.^[37]

Theoretical considerations

RnCOMT and other mammalian COMTs have been explored extensively for the methylation of different catechol derivatives, and the availability of many different structures with a plethora of ligands make it an interesting enzyme to explore its ability to methylate at sulfur atoms. To the best of our knowledge no cases of *S*-methylation have been reported for *RnCOMT* to date; nevertheless, mechanistically it should be possible. The pK_a value of phenols is higher than that of the corresponding thiophenols (for example phenol $pK_a=9.9$; thiophenol $pK_a=6.2$).^[38,39] Likewise, Mg^{2+} in combination with the active site lysine acting as a base (K_{144} in *RnCOMT*) should be able to generate the thiolate instead of the phenolate nucleophile for the methylation (Figure 2). Due to the considerably lower pK_a value of thiophenol (6.2) compared to catechol (9.45 for the first deprotonation), it might also be possible to deprotonate thiophenol or similar compounds with only one thiol/hydroxyl substituent, that do not resemble the catechol structure; a prerequisite for this would be a suitably tight binding mode. Dimethylation of catechols has been observed for the closely related *MxSafC* from *Myxococcus xanthus*.^[21]

Recently, many of the clinically approved COMT inhibitors including a 5-substituted-3-nitrocatechol ring as a pharmacophore, were shown to form a quaternary complex COMT/SAM/ Mg^{2+} /inhibitor. For example, the crystal structure of *RnCOMT* with the catechol derivative 6-(4-fluorophenyl)quinazolin-8-ol, which does not have a substitution in the 3-position (PDB ID: 5P9Z), showed that the Mg^{2+} cofactor can be coordinated by only one hydroxyl group. The hydroxyl group and the nitrogen atom inside the ring chelate the active site Mg^{2+} ion completing the octahedral complex around the Mg^{2+} without another hydroxyl group (Figure 3). In a comparison with many other active pharmaceutical ingredients (API) acting as inhibitors of MTs in general and *RnCOMT* in particular, it was demonstrated that these APIs fit well into the active site and bind tightly to *RnCOMT* even if they have only one hydroxyl group, suggesting that also a single thiol might suffice.

For the CaOMT group, the enzyme from *C. roseus* already presents an example for *S*-methylation,^[30] and due to the differences in binding and mechanism, the enzymes do not require the catechol moiety but also accept compounds with

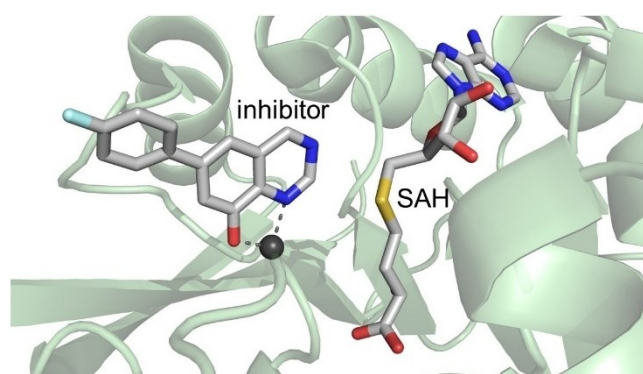


Figure 3. Representation of the catalytic site of an *RnCOMT* structure (5P9Z) co-crystallized with SAH and the inhibitor 6-(4-fluorophenyl)quinazolin-8-ol. The inhibitor is coordinately bound to the Mg^{2+} ion in the catalytic site by one hydroxyl group and one nitrogen atom in the aromatic ring.

just one hydroxyl group.^[29,40] The question remains if this can be extended to thiol groups.

In the present study, we show that representatives of both groups (COMT and CaOMT) indeed accept thiols as substrates, and discuss possible molecular reasons and implications for metabolism and application.

Results and Discussion

To test the hypothesis that OMTs are able to convert not only catechols and phenols, but also the corresponding thiophenols, we used an established linear in situ SAM supply system. SAM is generated from ATP and L-methionine. The by-product of the MT reaction (SAH) is removed by enzymatic cleavage forming adenine and *S*-ribosyl-L-homocysteine (Figure 6a) to prevent MT inhibition through the by-product SAH.^[5] First tests showed that *RnCOMT* indeed accepted a thiol containing substrate; however, most thiol compounds are only partly soluble in the aqueous buffer system. To introduce a homogeneous reaction system, we tested water miscible organic co-solvents. Thiosalicylic acid (1a) was chosen as model substrate for our investigations due to its good separation on HPLC. All seven solvents tested were tolerated by the enzymes used in the methylation cascade (Figure 4). Reactions without co-solvents, using only buffer showed the lowest conversion numbers, exemplarily shown for *RnCOMT* with 43% of product formation. All solvents tested led to product formation of over 89%. Eventually, acetonitrile, leading to 93% substrate methylation, was chosen as co-solvent in further experiments, also because of its compatibility with the HPLC analysis conditions (ACN/water).

Similarly, pH, buffer, the influence of $MgCl_2$ and temperature on the activity of the *RnCOMT* were investigated and optimized; as was the effect of the feedback inhibition by SAH on *RnCOMT* by testing the enzyme in presence and absence of a methyl thioadenosine/SAH nucleosidase from *E. coli* (*EcMTAN*) (Figure SI-3; Figure SI-4). Assays for *S*-methylation (in the three-enzyme cascade) were eventually performed with 5 mM thiol substrate dissolved in acetonitrile (end concentration 5% v/v),

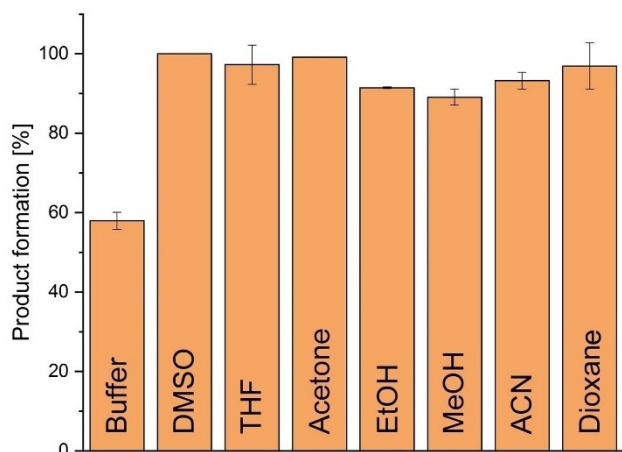


Figure 4. Co-solvent screening using thiosalicylic acid (**1a**) with *RnCOMT* as model system. Thiol compounds show low solubility under aqueous conditions. The impact of different co-solvents (5% v/v) on the enzymatic cascade used in this study was tested in comparison to the reaction in the buffer system only. The error bars represent the standard deviation of replicating the enzymatic reactions. The reaction without any co-solvents led to low conversion under 50%. All of the used organic solvents led to comparable conversion of over 89%.

5 mM ATP and L-methionine in 50 mM KP_i buffer (pH 7.5) containing 20 mM $MgCl_2$ and 50 mM KCl, at 37 °C, 800 rpm for 20 h.

As already seen in the preliminary tests with *RnCOMT*, **1a** was methylated with excellent selectivity. No formation of the ester on the carboxylic group was observed. The methyl transfer onto the sulfur was confirmed by HPLC analysis using commercially available standards, followed by LC–MS analysis confirming the mass of 2-(methylthio)benzoic acid (**2a**) (Figure SI–5). With *RnCOMT*, smooth conversion of the starting material into the product was observed with yields of 92% after 4 h (Figure 5).

To probe whether other OMTs can carry out *S*-methylation the reaction was also performed with the COMT from *Myxococcus xanthus* (*MxSafC*),^[24] and a metal-independent OMT

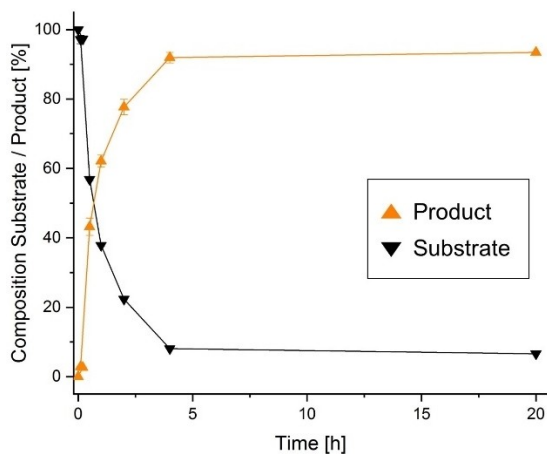


Figure 5. Time course of *RnCOMT* catalyzed reaction with **1a**. Samples were taken after 0.1, 0.2, 0.5, 1, 2, 4, and 20 h. After 4 h 92% of the substrate (black) is converted to the methylated product (orange).

from *Prunus persica* (*PpCaOMT*) involved in lignin biosynthesis, methylating caffeate in plants.^[29] Both enzymes substantially converted **1a** to **2a**. *MxSafC* formed about 26% of the *S*-methylated product **2a** within 20 h. In the reaction catalyzed by *PpCaOMT*, there was no substrate left after 20 h (Figure 6b). Compared to COMT enzymes, CaOMTs feature another mechanism for methylation and do not require coordination of the substrate by a cation in the active site. In this enzyme family, a histidine is known to act as the catalytic base, deprotonating the hydroxyl group for the following methylation step. So far, only *O*-methylation has been reported for *PpCaOMT*.^[29] Since a metal ion is not required for substrate coordination in the active site and the main step of the methylation reaction is deprotonating the nucleophile, it should be possible to use substrates with lower pK_a values compared to hydroxyl containing substrates to reach an enzymatic methylation transfer. Comparing the amino acid sequence of *PpCaOMT* with the reported SMT *CrSMT1* shows a high identity of 59% (Figure SI–2).

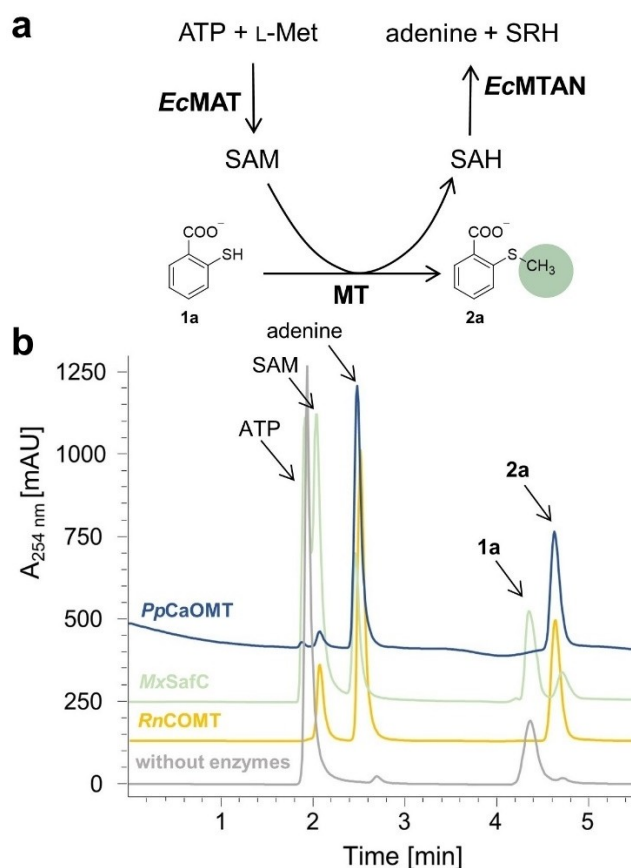


Figure 6. a: Three-enzyme cascade used for substrate methylation. ATP and L-Met are used for SAM formation, catalyzed by the MAT enzyme. The methyl group of SAM is transferred onto the substrate (here **1a**). SAH, the byproduct of the reaction is cleaved into adenine and SRH (*S*-ribosyl-L-homocysteine) by the MTAN enzyme to prevent inhibition effects on the methylation reaction by SAH. b: HPLC chromatograms of the methylation reaction of **1a** to **2a** catalyzed by three different MTs compared to the negative control without enzymes (grey). In the *RnCOMT* reaction (yellow), there was no substrate left after 20 h. In the *PpCaOMT* reaction (blue), only small amounts of the substrate are left, while in the reaction using *MxSafC* (green), **1a** was only partially converted.

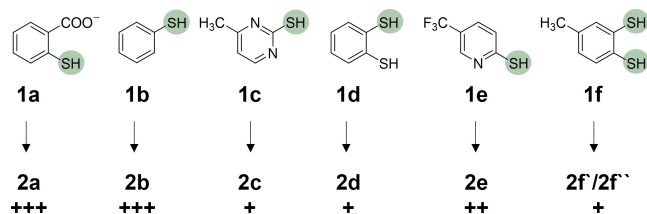


Figure 7. All tested and accepted aromatic substrates using *RnCOMT* in the three-enzyme methylation cascade; **1a**: thiosalicylic acid, **1b**: thiophenol, **1c**: 4-methylpyrimidine-2-thiol, **1d**: 1,2-dithiophenol, **1e**: 5-(trifluoromethyl)pyridine-2-thiol, **1f**: 4-methylbenzene-1,2-dithiol. The thiol group, acting as the nucleophile is highlighted in green. For substrate **1f** a formation of two different products (**2f**/**2f'**) was observed. Degree of conversion: + = modest, ++ = average, +++ = good. See also SI, subsection "Chromatograms".

After having successfully shown *S*-methylation using OMTs, we chose *RnCOMT* as a model enzyme for tests with other thiols. The results of the substrate screening are summarized in Figure 7 and Table SI-2.

The aromatic sulfhydryl-containing compounds, thiophenol (**1b**), 4-methylpyrimidine-2-thiol (**1c**), 1,2-dithiophenol (**1d**), 5-(trifluoromethyl)pyridine-2-thiol (**1e**), and 4-methylbenzene-1,2-dithiol (**1f**) exhibited modest to good levels of methylation after 20 h. Substrates and corresponding products were confirmed by HPLC (**1a**–**1c**) or GC-MS analysis (**1d**–**1f**). For substrate **1f** *S*-methylation at both thiol groups was observed: the results showed that *RnCOMT* produced a mix of products. Aliphatic thiols (thioglycolic acid, propane-1,3-dithiol and 3-mercapto-1-propanol) that were also tested in the study of *CrSMT1*^[30] were not accepted as substrates by *RnCOMT* (data not shown).

To get more insight in the mode of substrate stabilization, we performed docking studies with *RnCOMT* and two selected thiol substrates. Protein ligand interactions of *RnCOMT* with the thiol compounds **1a** and **1d** revealed several stabilizing factors holding each substrate in the right position for the methylation reaction [Docking score for **1a**: –6.35; **1d**: –5.85 (Figure 8)].

The negatively charged oxygen from the carboxyl group of **1a** can coordinatively bind to the Mg^{2+} ion in the active site. K_{144} forms a hydrogen bond with the carboxylate. The positive charge of K_{144} also supports the stabilization by electrostatic interactions with the carboxylate and/or thiolate. K_{144} is known as the catalytic base of *RnCOMT*, interacting with catechol compounds in a similar way.^[14] Additionally, a π - π stacking interaction with an orthogonal arrangement of W_{38} and the aromatic ring of the substrates was found. The distance between the substrate (center of the aromatic ring) and W_{38} (center of the six-membered ring) is between 5.3 (**1d**)–5.5 Å (**1a**). In this formation, the thiol groups of **1a** and **1d** are oriented towards the methyl group of the cofactor with a distance of 3.9 Å. Considering the protonation state under physiological conditions (pH 7.5), the thiol group of **1a** can partly be deprotonated making the negatively charged sulfur a good nucleophile ($pK_aSH=9.52$; salicylic acid $pK_aOH: 13.29$).^[41,42] For catechols, the pK_a values of the hydroxyl groups differ by around four units making the second hydroxyl group less acidic ($pK_{a1}=9.14$; $pK_{a2}=13.8$).^[43] This can be transferred to thiocatechols resulting in substrate **1d** to be deprotonated once. Distances between the cofactor and methyl acceptor in MTs vary. I.e., the hydroxyl group of the inhibitor in 1H1D shows a distance of 2.8 Å towards the cofactor methyl group. A structure of a CaOMT, co-crystallized with SAH and the methylated

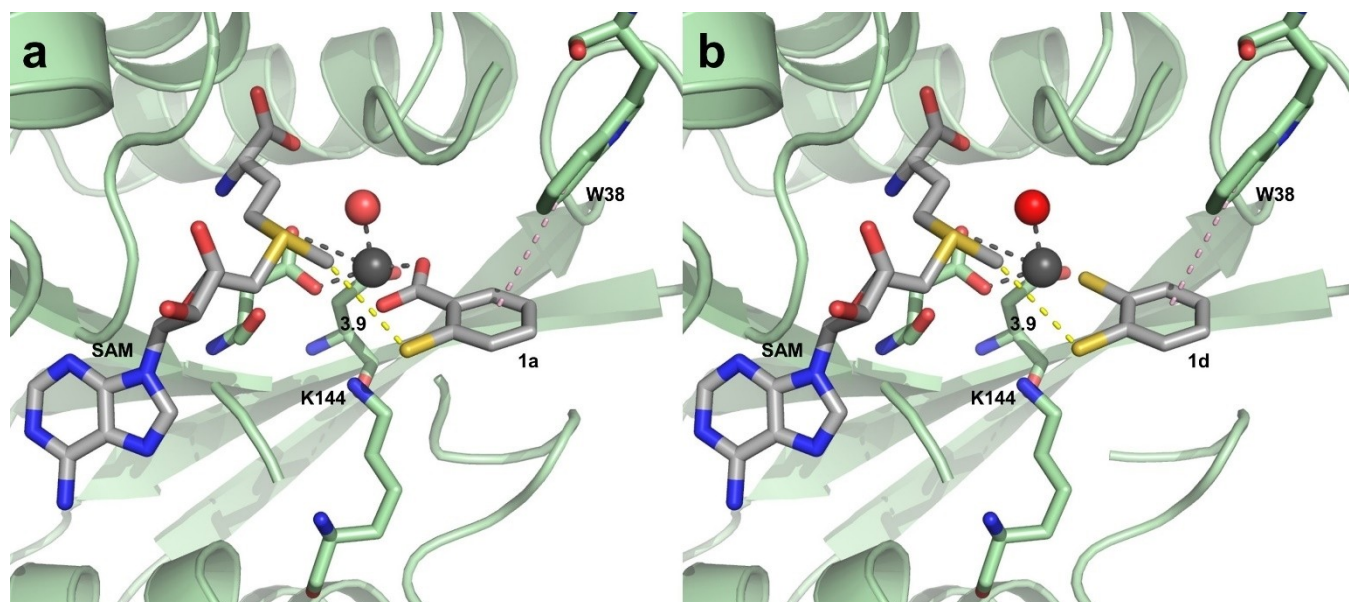


Figure 8. Docking results using a crystal structure of *RnCOMT* (1H1D) with two different thiol substrates (a: **1a**; b: **1d**). The crystal structure contained three ligands; SAM, Mg^{2+} and an enzyme inhibitor: 1-(3,4-dihydroxy-5-nitrophenyl)-3-{4-[3-(trifluoromethyl)phenyl] piperazin-1-yl}propan-1-one. Before docking experiments, the inhibitor was removed while SAM and the cation remained in the active site. Coordinative interactions between Mg^{2+} (grey sphere), a water molecule (red sphere) and **1a** are represented in grey. For both substrates **1a** and **1d**, there was a π - π stacking interaction found between the aromatic ring of the substrate and a tryptophan residue in position 38 (light pink dots). The distance between the substrate thiol and methyl group of the cofactor is presented in yellow, showing a distance of 3.9 Å making a nucleophilic attack possible. The docking score for **1a** was –6.35 and for **1d** –5.85.

compound (1KYZ) reaches a gap of 5.9 Å between the sulfur and the methyl group carbon.^[40] Therefore, a nucleophilic attack coming from a thiol with distances in between this range should be conceivable, leading to the *S*-methylated product. Because of the larger atomic radius of sulfur atoms compared to oxygen atoms, the S–C gap should be larger than O–C. For docking calculations, the structure was minimized, with heavy atoms converging to RMSD 0.3 Å. Distances between the prepared structure and the inhibitor, as well as the docked substrates were compared. The hydroxyl group of the inhibitor showed a distance of 2.9 Å to the carbon of the SAM methyl group. The gap between the thiol group of **1a/1d** and the methyl group of SAM was 3.9 Å, extending the distance by 1 Å for the larger sulfur atom (compared to the oxygen). As positive control for the thiol docking experiment, we redocked the co-crystallized inhibitor of the used crystal structure as well, reaching a docking score of –7.36.

Conclusions

Here, we showed that, in addition to CaOMTs such as *CrSMT1*, also COMTs accept thiophenols as substrates in addition to their (physiological) phenol- or catechol substrates. In addition to the new functional insights, SAM-dependent MTs are constantly further developed to serve as biocatalysts in technical applications. The possibility for *S*-methylation will add to the diversity of products accessible; the regioselective methylation of dithiols further adds to the versatility of this reaction.

Furthermore, the results obtained here will be interesting for the field of human metabolism and medicinal chemistry. *S*-methylation of cytostatic drugs in humans have already been reported.^[37] The amino acid sequence of human COMT (*HsCOMT*) is 79% identical (91% similar) to *RnCOMT*. It is therefore likely that *HsCOMT* is also capable of thiol methylation. The physiological role of COMT in mammals is the inactivation by methylation of catecholamine neurotransmitters (e.g. dopamine) and catechol hormones (e.g. 2-hydroxyestradiol). The newly discovered *S*-methylation activity of COMT enzymes may thus have physiological implications, e.g., for drug metabolism or metabolism of endogenous aromatic thiols.

Experimental Section

Materials

All chemicals were purchased in the highest purity available from Sigma Aldrich if not reported otherwise. Buffer ingredients, as well as cultivation media were obtained by VWR and Carl Roth.

Cloning and Protein Production

All used plasmids have been described previously.^[5,24,29]

E. coli BL21-Gold(DE3) cells were transformed with plasmids. A colony was incubated in 5 mL LB medium, containing kanamycin (50 µg·mL^{–1}) overnight at 37 °C, 170 rpm. The preculture (1%) was

added to 400 mL LB medium, containing kanamycin (50 µg·mL^{–1}) and incubated at 37 °C, 170 rpm until the OD₆₀₀ was between 0.5–0.7. After, isopropyl-β-D-thiogalactopyranoside (IPTG) was added (0.25 mM) for the induction of overexpression. The flasks were kept at 20 °C, 140 rpm for 20 h for the enzyme overproduction. Cells were harvested the next day by centrifugation (4 °C, 7.800 g) for 20 min and stored until purification at –20 °C.

Protein Purification

Pellets were resuspended in lysis buffer (40 mM Tris-HCl, pH 8, 100 mM NaCl, 10% (w/v) glycerol; 4 mL·g^{–1}). The lysis was performed using a Branson Sonifier 250 (duty cycle 50%, 5·30 s with 30 s break within). The lysed cells were centrifuged for 40 min (24.900 g) at 4 °C. The supernatant, containing the soluble enzyme was applied to the nickel-NTA column being washed with 30 mL lysis buffer containing 10 mM imidazole and eluted using 20 mL lysis buffer with 250 mM imidazole. Afterwards, the imidazole was removed using PD-10 columns (GE Healthcare Life Science, Little Chalfont, UK) according to the manufacturer's protocol. Protein concentration was determined at 280 nm with a NanoDrop 2000 (Thermo Fisher Scientific, Waltham, MA, USA). The molecular mass, as well as the extinction coefficient were calculated with ExPASy ProtParam.^[44]

Assays

Assays were performed at least in duplicate. The reaction buffer was KP_i (50 mM; pH 8) buffer, containing 20 mM MgCl₂ and 50 mM KCl. 5 mM substrates [ATP; L-methionine, and methyl acceptor (**1a–1f**, 100 mM stock solution in acetonitrile)] were added to the reaction. 12 µM *EcMAT*, 20 µM *MT*, and 3 µM *EcMTAN* were used. Samples were incubated at 37 °C, 800 rpm for 20 h. Negative control reactions were performed without the enzymes under the same reaction conditions. Enzymes were removed by precipitation with perchloric acid [2.5%, followed by spin filtration (0.45 µm) immediately before analysis]. Samples were shock-frozen in liquid nitrogen and stored until analysis using the following procedures. For screening of optimal conditions (e.g., temperature, buffer salt, co-solvent), the assay was adjusted correspondingly (see also SI Figure captions).

HPLC Analysis

HPLC analysis was used for the detection of substrates **1a–1c** and the corresponding methylated products. Samples were measured with a Shimadzu HPLC system on a C18 column (XTerra RP18 5 µm 4.6×150 mm). The column oven temperature was kept at 26 °C. The injection volume was 2 µL. Absorption was measured between 190–400 nm using a UV detector. The elution gradient was a mixture of sodium acetate 40 mM, pH 4.2 (**A**) and acetonitrile (**B**). 0–1 min 0% **B**, 1–5 min 0% to 80% **B**, 5–10 min 80% **B**, 10–11 min 80% to 0% **B**. The flow rate was 1 mL·min^{–1}.

Quantitative assays were calculated from the substrate and product AUC.

LC-MS Analysis

Mass spectrometric analysis was performed using an ACQUITY UPLC chromatography system (Waters, UK) coupled online to a high-resolution Orbitrap mass spectrometer (Q-Exactive Focus, Thermo Fisher Scientific, Germany). For chromatographic separation, a reverse phase separation column (ACQUITY UPLC BEH C18, 2.1×100 mm, 1.7 µm, Waters UK) was operated at room temper-

ature using H₂O plus 0.1% formic acid as mobile phase A, and acetonitrile plus 0.1% formic acid as mobile phase B. A gradient was maintained at 250 μ L/min at 3% B over 2 minutes. Solvent B was then increased to 80% over 30 minutes, before equilibrating back to the starting conditions. The mass spectrometer was operated alternating in full scan and PRM mode. Full scan was acquired from 80–500 m/z in ESI negative mode (–2.2 kV) at a resolution of 70 K. Additional parallel reaction monitoring was performed on expected parent masses. Peak isolation was performed using a 2.0 m/z isolation window. Fragmentation was performed at a NCE of 26, where fragment ions were acquired at a resolution of 35 K, using automatic max IT and an AGC target of 2e5. Raw data were analyzed using XCalibur 4.1 (Thermo Fisher Scientific, Germany) and the GNPS LC–MS dashboard (<https://gnps-lcms.ucsd.edu/>). The mass spectrometer was calibrated using the Pierce™ LTQ ESI positive ion calibration solution (Thermo Fisher Scientific, Germany).

GC-MS Analysis

200 μ L of the samples containing substrate **1d–1f** and their corresponding products were extracted (2·100 μ L ethyl acetate). After centrifugation, the phases were separated. The organic phase was dried with MgSO₄ and centrifuged for 1 min, followed by GC-MS analysis using a CP sil 5CB/FVF-1 ms column (25 m×0.25 mm×0.4 μ m). Column oven program: T_{0 min} = 60 °C; T_{5 min} = 60 °C; T_{10 min} = 325 °C; T_{20 min} = 325 °C. Total flow rate: 20 mL·min^{–1}. Injector temperature: 250 °C. Detector temperature: 325 °C. Split ratio: 20:1. Carrier gas: N₂.

Docking Experiments

The crystal structure of RnCOMT (PDB: 1H1D) was prepared using the Protein Preparation Wizard.^[45] This was done in order to obtain all-atom structure with correct bond orders and formal charges to be used for docking. The steps performed during protein preparation included adding hydrogens, assigning bond orders, correcting charges and optimizing the hydrogen bond network. Strained bond angles and clashes were relaxed by running a restrained minimization (converge heavy atoms to RMSD 0.3 Å) of the protein. The force field used for minimization was OPLS3e.^[46] The cofactor (SAM), metal ion (Mg²⁺) and the water molecule coordinating with Mg²⁺ were kept in the pocket.

All ligands docked were prepared using the tool LigPrep (Schrödinger Release 2020–3: LigPrep, Schrödinger, LLC, New York, NY, 2020) in order to obtain accurate energy minimized 3D structures. Ligands were docked using the Glide Docking protocol available in the Schrödinger Software Suite.^[47] Ligands were flexibly docked and scored using the Standard-Precision (SP) Glide scoring function. No constraints were used during docking.

Supporting Information

Electronical supporting information is accessible via the following link:

Acknowledgements

The authors are grateful for generous financial support from ERA-CoBiotech (grant 053.80.737; BioDiMet), E.J., and J.N.A. acknowledge funding from the European Research Council

(grant number 716966), as well as from the Deutsche Forschungsgemeinschaft (RTG1976). We thank Adelheid Nagel for technical support and Raspudin Saleem-Batcha bioinformatic-related discussions.

Conflict of Interests

The authors declare no conflict of interest.

Data Availability Statement

The data that support the findings of this study are available from the corresponding author upon reasonable request.

Keywords: aromatic thiols · caffeate OMT · catechol OMT · chemoselectivity · S-methylation

- [1] E. J. Barreiro, A. E. Kümmerle, C. A. M. Fraga, *Chem. Rev.* **2011**, *111*, 5215–5246.
- [2] H. Schönherr, T. Cernak, *Angew. Chem. Int. Ed.* **2013**, *52*, 12256–12267.
- [3] E. Fossati, A. Ekins, L. Narcross, Y. Zhu, J.-P. Falueyret, G. A. W. Beaudoin, P. J. Facchini, V. J. J. Martin, *Nat. Commun.* **2014**, *5*, 3283.
- [4] E. Abdelraheem, B. Thair, R. F. Varela, E. Jockmann, D. Popadić, H. C. Hailes, J. M. Ward, A. M. Iribarren, E. S. Lewkowicz, J. N. Andexer, P. Hagedoorn, U. Hanefeld, *ChemBioChem* **2022**, *23*, DOI 10.1002/cbic.202200212.
- [5] J. Siegrist, S. Aschwanden, S. Mordhorst, L. Thöny-Meyer, M. Richter, J. N. Andexer, *ChemBioChem* **2015**, *16*, 2576–2579.
- [6] S. Mordhorst, J. Siegrist, M. Müller, M. Richter, J. N. Andexer, *Angew. Chem. Int. Ed.* **2017**, *56*, 4037–4041.
- [7] D. Popadić, D. Mhaindarkar, M. H. N. Dang Thai, H. C. Hailes, S. Mordhorst, J. N. Andexer, *RSC Chem. Biol.* **2021**, DOI:10.1039/D1CB00033K.
- [8] L. Gericke, D. Mhaindarkar, L. C. Karst, S. Jahn, M. Kuge, M. K. F. Mohr, J. Gagsteiger, N. V. Cornelissen, X. Wen, S. Mordhorst, H. J. Jessen, A. Rentmeister, F. P. Seebeck, G. Layer, C. Loenarz, J. N. Andexer, *ChemBioChem* **2023**, *24*, e202300133. doi.org/10.1002/cbic.202300133.
- [9] C. Liao, F. P. Seebeck, *Nat. Catal.* **2019**, *2*, 696–701.
- [10] L. L. Bengel, B. Aberle, A.-N. Egler-Kemmerer, S. Kienzle, B. Hauer, S. C. Hammer, *Angew. Chem. Int. Ed.* **2021**, *60*, 5554–5560.
- [11] S. E. Wu, W. P. Huskey, R. T. Borchardt, R. L. Schowen, *Biochemistry* **1983**, *22*, 2828–2832.
- [12] M. Selva, A. Perosa, *Green Chem.* **2008**, *10*, 457.
- [13] Y. Chen, *Chem. Eur. J.* **2019**, *25*, 3405–3439.
- [14] P. T. Männistö, S. Kaakkola, *Pharmacol. Rev.* **1999**, *51*, 593–628.
- [15] J. Axelrod, R. Tomchick, *J. Biol. Chem.* **1958**, *233*, 702–705.
- [16] S. Senoh, C. R. Creveling, S. Udenfriend, B. Witkop, *J. Am. Chem. Soc.* **1959**, *81*, 6236–6240.
- [17] J. W. Daly, J. Axelrod, B. Witkop, *J. Biol. Chem.* **1960**, *235*, 1155–1159.
- [18] H. L. Schubert, R. M. Blumenthal, X. Cheng, *Trends Biochem. Sci.* **2003**, *28*, 329–335.
- [19] J. Vidgren, L. A. Svensson, A. Liljas, *Nature* **1994**, *368*, 354–358.
- [20] T. Lotta, J. Vidgren, C. Tilgmann, I. Ulmanen, K. Melen, I. Julkunen, J. Taskinen, *Biochemistry* **1995**, *34*, 4202–4210.
- [21] F. Subrizi, Y. Wang, B. Thair, D. Méndez-Sánchez, R. Roddan, M. Cárdenas-Fernández, J. Siegrist, M. Richter, J. N. Andexer, J. M. Ward, *Angew. Chem.* **2021**, *133*, 18821–18827.
- [22] D. R. Thakker, C. Boehlert, K. L. Kirk, R. Antkowiak, C. R. Creveling, *J. Biol. Chem.* **1986**, *261*, 178–184.
- [23] B. J. C. Law, M. R. Bennett, M. L. Thompson, C. Levy, S. A. Shepherd, D. Leys, J. Micklefield, *Angew. Chem.* **2016**, *128*, 2733–2737.
- [24] J. Siegrist, J. Netzer, S. Mordhorst, L. Karst, S. Gerhardt, O. Einsle, M. Richter, J. N. Andexer, *FEBS Lett.* **2017**, *591*, 312–321.
- [25] C. P. Joshi, V. L. Chiang, *Plant Mol. Biol.* **1998**, *37*, 663–674.
- [26] G. V. Louie, M. E. Bowman, Y. Tu, A. Mouradov, G. Spangenberg, J. P. Noel, *The Plant Cell* **2010**, *22*(15), 4114–4127.

- [27] D. R. Gang, N. Lavid, C. Zubieta, F. Chen, T. Beuerle, E. Lewinsohn, J. P. Noel, E. Pichersky, *Plant Cell* **2002**, *14*, 505–519.
- [28] B. Rohde, J. Hans, S. Martens, A. Baumert, P. Hunziker, U. Matern, *Plant J.* **2008**, *53*, 541–553.
- [29] E. Jockmann, F. Subrizi, M. K. F. Mohr, E. M. Carter, P. M. Hebecker, D. Popadić, H. C. Hailes, J. N. Andexer, *ChemCatChem*. **2023**, e202300930.
- [30] H. Coirer, G. Schröder, E. Wehinger, C.-J. Liu, J. P. Noel, W. Schwab, J. Schröder, *Plant J.* **2006**, *46*, 193–205.
- [31] J. D. Finkelstein, B. J. Harris, W. E. Kyle, *Arch. Biochem. Biophys.* **1972**, *153*, 320–324.
- [32] S. S. Szegedi, C. C. Castro, M. Koutmos, T. A. Garrow, *J. Biol. Chem.* **2008**, *283*, 8939–8945.
- [33] C. W. Goulding, D. Postigo, R. G. Matthews, *Biochemistry* **1997**, *36*, 8082–8091.
- [34] C. R. Vinci, S. G. Clarke, *J. Biol. Chem.* **2010**, *285*, 20526–20531.
- [35] A. M. Drotar, R. Fall, *Plant Cell Physiol.* **1985**, *26*, 847–854.
- [36] R. M. Weinshilboum, D. M. Otterness, C. L. Szumlanski, *Annu. Rev. Pharmacol. Toxicol.* **1999**, *39*, 19–52.
- [37] C. W. Keuzenkamp-Jansen, P. A. J. Leegwater, R. A. De Abreu, M. A. H. Lambooy, J. P. M. Böklerink, J. M. F. Trijbels, *J. Chromatogr. B. Biomed. Sci. App.* **1996**, *678*, 15–22.
- [38] M. Djebbar, F. Djafri, M. Boucekara, A. Djafri, *Appl. Water Sci.* **2012**, *2*, 77–86.
- [39] K. N. Dalby, W. P. Jencks, *J. Chem. Soc. Perkin Trans. 2* **1997**, 1555–1564.
- [40] C. Zubieta, P. Kota, J.-L. Ferrer, R. A. Dixon, J. P. Noel, *Plant Cell* **2002**, *14*, 1265–1277.
- [41] A. M. Abdel-Mawgoud, R. Abdel-Hamid, *Chemical Monthly* **1986**, *118*, 1219–1223.
- [42] T. Baba, T. Matsui, K. Kamiya, M. Nakano, Y. Shigeta, *Int. J. Quantum Chem.* **2014**, *114*, 1128–1134.
- [43] V. M. Nurchi, T. Pivetta, J. I. Lachowicz, G. Crisponi, *J. Inorg. Biochem.* **2009**, *103*, 227–236.
- [44] E. Gasteiger, C. Hoogland, A. Gattiker, S. Duvaud, M. R. Wilkins, R. D. Appel, A. Bairoch, in *Proteomics Protoc. Handb.* (Ed.: J. M. Walker), Humana Press, Totowa, NJ, **2005**, pp. 571–607.
- [45] G. Madhavi Sastry, M. Adzhigirey, T. Day, R. Annabhimoju, W. Sherman, *J. Comput.-Aided Mol. Des.* **2013**, *27*, 221–234.
- [46] K. Roos, C. Wu, W. Damm, M. Reboul, J. M. Stevenson, C. Lu, M. K. Dahlgren, S. Mondal, W. Chen, L. Wang, R. Abel, R. A. Friesner, E. D. Harder, *J. Chem. Theory Comput.* **2019**, *15*, 1863–1874.
- [47] R. A. Friesner, J. L. Banks, R. B. Murphy, T. A. Halgren, J. J. Klicic, D. T. Mainz, M. P. Repasky, E. H. Knoll, M. Shelley, J. K. Perry, D. E. Shaw, P. Francis, P. S. Shenkin, *J. Med. Chem.* **2004**, *47*, 1739–1749.

Manuscript received: September 29, 2023

Revised manuscript received: November 8, 2023

Accepted manuscript online: November 14, 2023

Version of record online: December 11, 2023